Journal of Medicinal Chemistry Article

J. Med. Chem. **2010,** *53,* 5759–5769 **5759**
DOI: 10.1021/jm100561b

Novel Thiosemicarbazones of the ApT and DpT Series and Their Copper Complexes: Identification of Pronounced Redox Activity and Characterization of Their Antitumor Activity

Patric J. Jansson,[†] Philip C. Sharpe,[‡] Paul V. Bernhardt,*[,‡,§] and Des R. Richardson*[,†,§]

[†]*Department of Pathology and Bosch Institute, University of Sydney, Sydney, NSW 2006, Australia, and* [‡]*Centre for Metals in Biology, School of Chemistry and Molecular Biosciences, University of Queensland, Brisbane, Qld 4072, Australia.* [§]*P.V.B. and D.R.R. contributed equally as senior authors.*

Received May 8, 2010

The novel chelators 2-acetylpyridine-4,4-dimethyl-3-thiosemicarbazone (**H**Ap44mT) and di-2-pyridylketone-4,4-dimethyl-3-thiosemicarbazone (**H**Dp44mT) have been examined to elucidate the structure−activity relationships necessary to form copper (Cu) complexes with pronounced antitumor activity. Electrochemical studies demonstrated that the Cu complexes of these ligands had lower redox potentials than their iron complexes. Moreover, the Cu complexes where the ligand/metal ratio was 1:1 rather than 2:1 had significantly higher intracellular oxidative properties and antitumor efficacy. Interestingly, the 2:1 complex was shown to dissociate to give significant amounts of the 1:1 complex that could be the major cytotoxic effector. Both types of Cu complex showed significantly more antiproliferative activity than the ligand alone. We also demonstrate the importance of the inductive effects of substituents on the carbonyl group of the parent ketone, which influence the $Cu^{II/I}$ redox potentials because of their proximity to the metal center. The structure−activity relationships described are important for the design of potent thiosemicarbazone Cu complexes.

Introduction

Many current chemotherapies remain ineffective against a variety of common and aggressive cancers, particularly solid tumors. Therefore, novel compounds that are able to selectively prevent cancer cell proliferation are essential to develop. Iron (Fe) chelators are an emerging class of ligands that show pronounced and selective antitumor activity in vitro and in vivo and can overcome resistance to standard chemotherapy.[1−8] This approach has been assessed because cancer cells show increased Fe requirements in comparison to their normal counterparts, leading to sensitivity to Fe depletion.[3,8−12] In fact, neoplastic cells express enhanced levels of the transferrin receptor 1 (TfR1[a])[13,14] and take up Fe from the serum Fe-binding molecule, transferrin, at a rapid rate.[10] Considering this, it is of interest that the well-known Fe chelators, desferrioxamine (DFO, Figure 1) and 3-aminopyridine-2-carboxaldehyde thiosemicarbazone (3-AP, Figure 1), have entered clinical trials for the treatment of a variety of malignancies.[7]

Cancer cells have also been shown to take up greater amounts of copper (Cu) than normal cells,[15,16] and Cu metabolism has been linked to angiogenesis[17] and metastasis.[18] Therefore, development of compounds that chelate Cu has become a therapeutic strategy showing significant promise.[18−20]

Recently, investigations from our laboratories have led to the development of a series of effective di-2-pyridylketone thiosemicarbazone (**H**DpT, Figure 1) chelators.[19,21] One of these chelators, di-2-pyridylketone-4,4-dimethyl-3-thiosemicarbazone (**H**Dp44mT, Figure 1), showed selective antitumor activity against a variety of aggressive human xenografts in nude mice.[21] For instance, following intravenous administration for 7 weeks (5 days/week), the net growth of an aggressive melanoma xenograft in **H**Dp44mT-treated mice was only 8% of that found for animals treated with the vehicle.[2,21]

Since the discovery of the selective antitumor activity of the **H**DpT series,[21] further studies have examined the effect of replacing the parent ketone of **H**DpT (di-2-pyridylketone) with 2-acetylpyridine, forming the 2-acetylpyridine thiosemicarbazone group of compounds (**H**ApT, Figure 1).[2,22] This has enabled variations in the activity due to N4 substituents to be separated from those due to the substituent attached to the imine nitrogen, i.e., 2-pyridyl (**H**DpT) and methyl (**H**ApT).[2,22] This approach has led to a potent group of compounds, where the ligand 2-acetylpyridine-4,4-dimethyl-3-thiosemicarbazone (**H**Ap44mT) has been shown to have high Fe chelation efficacy and antiproliferative activity.[23]

The mechanism of action of some chelators (e.g., the **H**DpT and **H**ApT series) is dependent not only on Fe chelation but also on redox-cycling of their Fe complexes to generate reactive oxygen species (ROS).[2,19] In their reduced (Fe^{II}) form, these complexes can react with molecular oxygen and

*To whom correspondence should be addressed. For P.V.B. (chemistry): phone, +61-7-3365-4266; fax, +61-7-3365-4299; e-mail, p.bernhardt@uq.edu.au. For D.R.R. (biology and chemistry): phone, +61-2-9036-6548; fax, +61-2-9036-6549; e-mail, d.richardson@med.usyd.edu.au.

[a] Abbreviations: 3-AP, 3-aminopyridine-2-carboxaldehyde thiosemicarbazone; BCS, bathocuproine disulfonate; BSO, buthione sulfoximine; **H**ApT, 2-acetylpyridine thiosemicarbazone; **H**Ap44mT, 2-acetylpyridine 4,4-dimethyl-3-thiosemicarbazone; DFO, desferrioxamine; $\mathbf{H_2}$DCF, 2′,7′-dichlorodihydrofluorescein; DCF, 2′,7′-dichlorofluorescein; **H**DpT, di-2-pyridylketone thiosemicarbazone; **H**Dp44mT, di-2-pyridylketone 4,4-dimethyl-3-thiosemicarbazone; GSH, glutathione; MTT, 1-(4,5-dimethylthiazol- 2-yl)-2,5-diphenyltetrazolium; PBS, phosphate buffered saline; ROS, reactive oxygen species; Tf, transferrin; TfR1, transferrin receptor 1; TM, tetrathiomolybdate.

Published on Web 07/02/2010

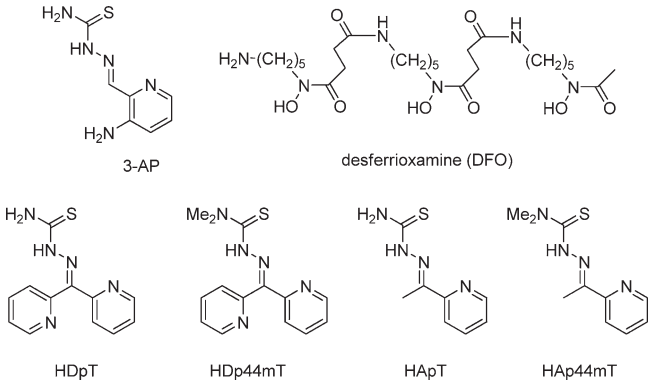

Figure 1. Line drawings of existing and novel chelators discussed herein.

the resulting ferric complexes may subsequently interact with cellular reductants.[24,25] This results in the catalytic generation of reactive oxygen species (ROS), e.g., hydroxyl radicals ($OH^{\bullet}$), leading to damage of essential biomolecules within cells.[24,25]

Interestingly, since the 1970s, Cu complexes of a great variety of ligands, such as thiosemicarbazones, imidazoles, and phosphines, have been proposed as potential anticancer agents.[26] More recently, this has expanded into other areas such as the role of Cu in neurodegenerative disorders and Cu-radioisotope-based imaging.[27,28] Further, the combination of Cu^{II} salts and specific Cu chelators has been shown to suppress proliferation of human cancer cells.[12,15] Indeed, these Cu complexes can interact with molecular oxygen and cellular oxidants and reductants, allowing Cu to redox-cycle between its mono- and divalent oxidation states.[16]

Considering this, and that **H**DpT and **H**ApT ligands form Fe and Cu complexes with redox activity,[29] in the current study, Cu complexes of the **H**DpT and **H**ApT chelators were synthesized and characterized. A particular focus of our work was the effect of the Cu/ligand stoichiometry, as it is known that Cu complexes are both highly labile and form more stable complexes than other divalent biometals such as Zn. We demonstrate that the 1:1 and 1:2 Cu/ligand complexes of **H**Ap44mT and **H**Dp44mT exhibit distinctly different chemical and biological properties and these differences can be rationalized on the basis of their structures and redox activity.

Results and Discussion

Synthesis and Structural Characterization. In previous investigations of the **H**DpT and **H**ApT series, our aim was to examine 1:2 metal/ligand (coordinately saturated) six-coordinate complexes. Indeed, we have characterized 1:2 complexes of the metal ions Mn^{II}, Fe^{II}, Fe^{III}, Co^{III}, Ni^{II}, Cu^{II}, and Zn^{II} with the **H**DpT analogues.[2,29] In these latter studies and with all other analogues we have assessed,[22,23,30] the ligands coordinate as NNS tridentate chelators and 6-coordinate 1:2 metal/ligand complexes are the result.

Since copper complexes are (i) particularly labile in their di- and monovalent oxidation states, (ii) redox active, and (iii) atypical in their preference for distorted (divalent) coordination geometries, they are much less structurally predictable than other first row transition metal complexes. Considering this, we were particularly interested to assess whether 1:1 Cu/ligand complexes could be isolated and if we could define any differences in physical and chemical properties that may be linked with a change in biological activity.

In our previous work,[29] we were able to isolate a bis-thiosemicarbazone Cu^{II} complex by reaction with excess thiosemicarbazone in the presence of base. The rather low solubility of the 1:2 Cu/ligand complex assisted in its isolation. In the crystallographically characterized example, $[Cu(Dp44mT)_2]$[29], a pair of trans donor atoms (pyridyl N and S) were quite distant from the metal, which is characteristic of the Jahn−Teller effect[31,32] (dashed coordinate bonds in Scheme 1). This typical 4 + 2 tetragonally elongated coordination geometry clearly destabilizes the ligand occupying the axial coordination sites and indicates the possibility of isolating the intermediate 1:1 complex.

In the present study, we were successful in isolating both 1:1 and 1:2 Cu/L complexes of **H**Ap44mT and **H**Dp44mT (the 1:2 Cu^{II}/**H**Dp44mT complex was reported by us previously[29]). The choice of $Cu(OAc)_2$ as the precursor offers the dual advantage of providing a base which is required to deprotonate the thiosemicarbazone prior to coordination and a competitive ligand that occupies the coordination site coplanar with the existing NNS chelator (Scheme 1). Under these conditions and in the absence of an excess of ligand, the 1:1 complexes of **H**Dp44mT and **H**Ap44mT were isolated.

The X-ray crystal structure of [Cu(Ap44mT)(OAc)] was determined, and the coordination geometry was shown to approximate square planar (Figure 2). A very weak axial interaction comes from an O-atom of the asymmetrically coordinated pseudobidentate acetate ligand (Cu−O2, 2.623(3) Å), while the equatorially bound O-atom is more strongly coordinated (Cu−O1, 1.954(2) Å). A water molecule is H-bonded to the more weakly coordinated acetate O-atom (Figure 2). The $Ap44mT^{-}$ anion coordinates in its ene−thiolate form, with N3−C8 exhibiting double bond and C8−S1 adopting single bond character (Table 2).

Under similar synthetic conditions reported for the complex $[Cu(Dp44mT)_2]$,[29] the analogous $[Cu(Ap44mT)_2]$ complex was isolated and its crystal structure was determined (Figure 3). The structure comprises two molecules in the asymmetric unit that both exhibit the same bond lengths and angles within experimental uncertainty. The geometry of the complex approximates tetragonally elongated octahedral, with one thiosemicarbazone anion coordinated more strongly than the other, as shown for molecule 1 in Figure 3.

EPR Spectroscopy. The d^9 Cu^{II} complexes, because of their lability, may exhibit significantly different solution and solid state structures. EPR spectroscopy is an ideal method for analyzing solution structures of Cu^{II} complexes, as variations in both the molecular g values and hyperfine coupling constants ($A_{x,y,z}$) are very sensitive to the coordination geometry.[32,33] Indeed, the 1:1 and 1:2 Cu/ligand complexes yielded distinctly different EPR spectra (Figure 4), which to a first approximation is a reflection of their crystallographically determined square planar and tetragonally elongated octahedral structures, respectively.

The spectra of both $[Cu(Ap44mT)_2]$ and its homologue $[Cu(Dp44mT)_2]$ clearly show the presence of at least two distinctly different species. Comparison with the spectra of the 1:1 complexes revealed that upon dissolution both $[Cu(Ap44mT)_2]$ and $[Cu(Dp44mT)_2]$ partially dissociate to afford the corresponding 1:1 Cu/ligand complexes. This is illustrated more clearly in Figure 5, where the observed EPR spectrum of $[Cu(Ap44mT)_2]$ is evidently a composite of the 1:2 and 1:1 Cu/ligand complexes, the latter simulated spectrum being obtained from [Cu(Ap44mT(OAc)] (see Supporting Information). In the absence of acetate in this case, a

Scheme 1

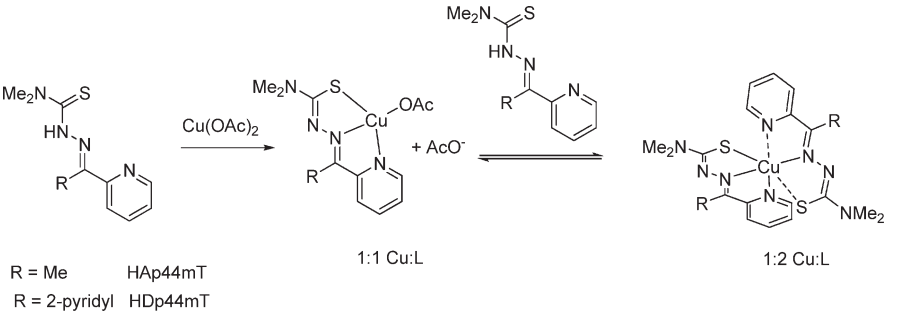

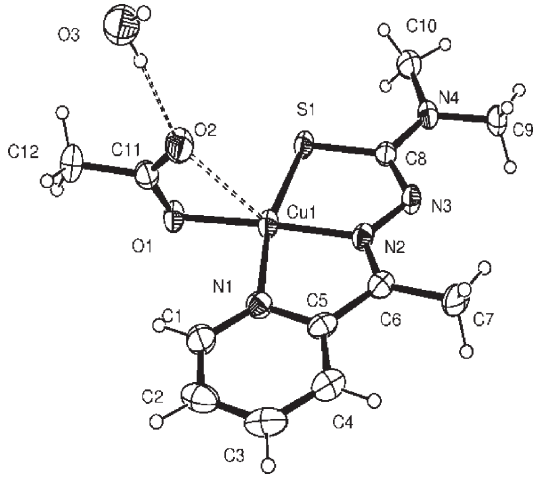

Figure 2. ORTEP view of $[Cu(Ap44mT)(OAc)]\cdot H_2O$ (30% probability ellipsoids). The weaker axial coordination of the acetate ligand is shown with a broken line as is the H-bond to the water molecule.

Table 1. Crystal Data

	$[Cu(Ap44mT)(OAc)]\cdot H_2O$	$[Cu(Ap44mT)_2]$
formula	$C_{12}H_{18}CuN_4O_3S$	$C_{20}H_{26}CuN_8S_2$
formula weight	361.90	506.15
crystal system	triclinic	monoclinic
space group	$P\bar{1}$ (No. 2)	$P2_1/c$ (No. 14)
color	brown	brown
a, Å	7.3442(4)	18.2621(5)
b, Å	9.1699(5)	29.593(1)
c, Å	12.1612(7)	8.7166(3)
α, deg	77.960(5)	
β, deg	82.399(5)	94.429(3)
γ, deg	76.310(5)	
V, Å^3	775.26(7)	4696.6(3)
T, K	293	293
Z	2	8
R1 (obs data)	0.0401	0.0441
wR2 (all data)	0.0693	0.0614
GOF	0.781	0.733
CCDC	775 627	775 628

DMF solvent molecule (also an O-donor) is anticipated to coordinate in the fourth coordination site of the putative square planar complex $[Cu(Ap44mT)(DMF)]^+$, but this should have little bearing on the spectrum relative to that of $[Cu(Ap44mT)(OAc)]$.

The same observation is found for the $[Cu(Dp44mT)_2]$ system (see bottom spectrum in Figure 4), and in fact, dissociation to the $[Cu(Dp44mT)(DMF)]^+$ complex is even more pronounced (note the larger proportion of the 1:1 complex than for $[Cu(Ap44mT)_2]$). On this basis, it is clear that upon dissolution, the 1:2 Cu/ligand complexes partially dissociate at millimolar concentrations (and presumably more so at micromolar concentrations) and the 1:1 complexes must be considered to be the major species under these conditions.

Table 2. Selected Bond Lengths (Å) and Angles (deg)

		$[Cu(Ap44mT)_2]^a$	
	$[Cu(Ap44mT)(OAc)]\cdot H_2O$	ligand A	ligand B
Cu−N1	2.014(3)	2.216(4)	2.238(3)
Cu−N2	1.943(3)	1.998(3)	2.011(3)
Cu−S1	2.253(1)	2.378(1)	2.487(1)
Cu−O1	1.954(2)		
N3−C8	1.328(4)	1.334(5)	1.323(4)
C8−S1	1.750(4)	1.706(4)	1.724(4)
N1−Cu−N2	80.9(1)	76.5(2)	76.4(1)
N1−Cu−S1	165.5(1)	157.1(1)	150.98(9)
N2−Cu−S1	84.6(1)	82.1(1)	79.9(1)
N2−Cu−O1	176.9(1)		

[a] Molecule 1 data only.

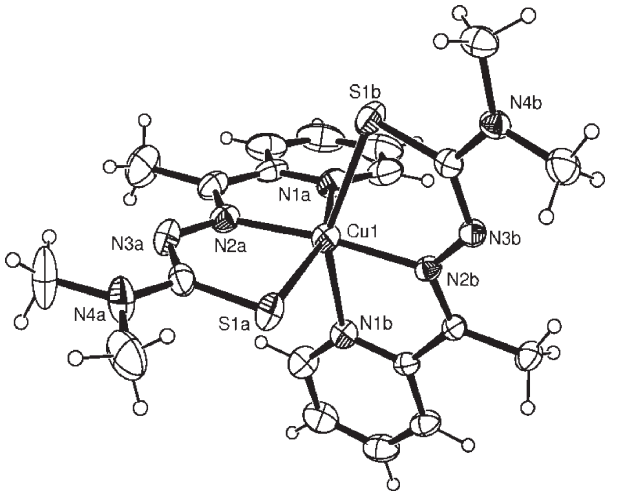

Figure 3. ORTEP view of one of the two $[Cu(Ap44mT)_2]$ molecules in the asymmetric unit (30% probability ellipsoids). The more tightly bound ligand (with "a" labels) is coordinated equatorially as drawn, while the axial Cu−S1B and Cu−N1b bond lengths are significantly elongated.

Electrochemistry. As redox activity has been linked with cytotoxicity of complexes of the thiosemicarbazones, particularly their Fe complexes,[2,22,23] we undertook an investigation into the effect of complex stoichiometry on their electrochemical properties (Figure 6). By use of cyclic voltammetry, the $Cu^{II/I}$ redox potentials were determined in a mixture of MeCN and water (7:3 v/v) to ensure sufficient solubility.

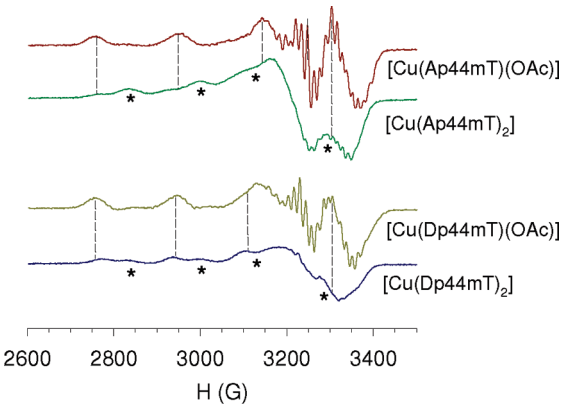

Figure 4. EPR spectra of the Cu^{II} complexes as 1 mM frozen DMF solutions. The vertical broken lines show major peaks due to the 1:1 Cu/ligand complex which are common to both spectra. The asterisks highlight peaks unique to the 1:2 Cu/ligand complex.

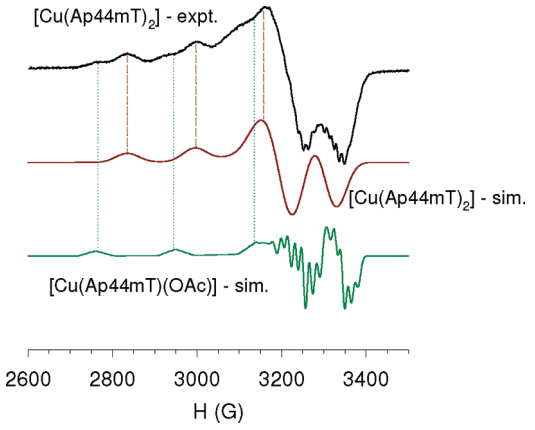

Figure 5. Experimental EPR spectrum of [Cu(Ap44mT)$_2$] (1 mM in DMF, top) and simulated EPR spectra of [Cu(Ap44mT)$_2$] (center) and [Cu(Ap44mT)(OAc)] (bottom) showing how the observed spectrum is a composite of these two species. Experimental conditions: $\nu = 9.301$ GHz, $T = 77$ K.

From inspection of Figure 6, it is apparent that the 1:2 Cu/ligand complexes are reduced at a potential ~400 mV more negative than their analogous 1:1 complexes. The electrochemistry is complicated, and the voltametric waves are only quasi-reversible. Also, more than one redox response is apparent, indicating a mixture of complexes is present. This mirrors the EPR results, and the minor higher potential responses in the [Cu(Dp44mT)$_2$] and [Cu(Ap44mT)$_2$] voltammograms are most likely due to partially dissociated complexes with a solvent molecule occupying the fourth coordination equatorial site in $[Cu(Dp44mT)(S)]^+$ and $[Cu(Ap44mT)(S)]^+$ (S = H_2O or MeCN).

Interestingly, the cyclic voltammograms of [Cu(Dp44mT)(OAc)] and [Cu(Ap44mT)(OAc)] also exhibit two responses characteristic of Cu complexes in different coordination environments. The most obvious explanation is substitution of the acetate ligand by solvent, and in fact, this was confirmed by sequential addition of NaOAc to the electrochemical cell to reverse this process in both cases. The example shown in Figure 7 is for the [Cu(Ap44mT)(OAc)] system, and the higher potential minor response from the solvated complex is suppressed as the concentration of acetate is raised.

Cu Complexes Participate in Fenton-Type Reactions in Vitro. Considering the electrochemical studies above

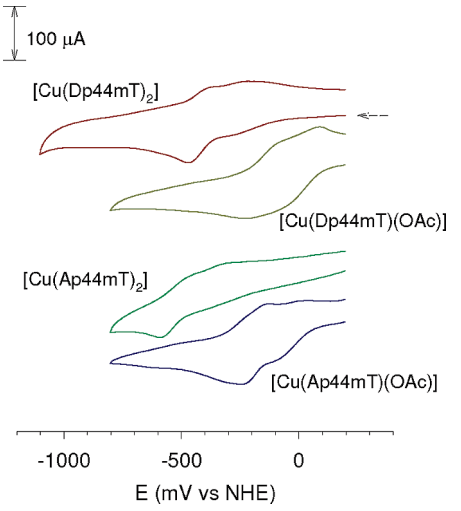

Figure 6. Cyclic voltammograms of the Cu complexes prepared in this investigation. All solutions were as 5 mM complexes dissolved in MeCN/H_2O (7:3). The sweep rate was 500 mV s^{-1}, and all sweeps were initiated in the direction of the arrow.

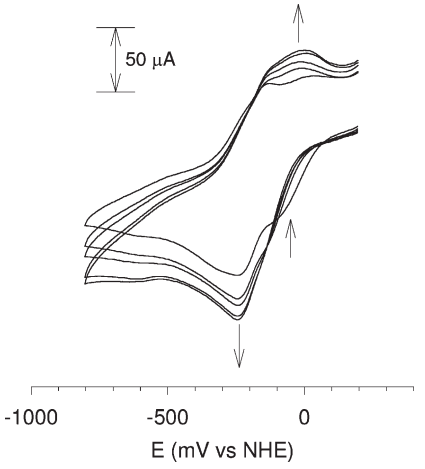

Figure 7. Cyclic voltammograms of [Cu(Ap44mT)(OAc)] (5 mM in H_2O/MeCN 3:7, 500 mV s^{-1} sweep rate) in the presence of additional concentrations of NaOAc (0, 4, 8, 12, and 16 mM in the direction of the arrows). Disappearance of the higher potential response around 0 mV vs NHE is coupled with formation of [Cu(Ap44mT)(OAc)] as the only species in solution.

(Table 1), if Cu redox cycles between its Cu^I and Cu^{II} redox states in the presence of oxygen, the single electron reduction of O_2 generating superoxide ($O_2^{\bullet -}$) is likely.[34] The hydroxyl radical ($OH^\bullet$) can also be directly formed from hydrogen peroxide (H_2O_2) and Cu^I in a way analogous to the reaction involving Fe^{II} and H_2O_2 (Fenton chemistry).[35−37] Both radicals can cause damage to biomolecules within cells.[34] These processes may play a role in the antitumor effects of these chelators through formation of intracellular redox-active Cu complexes.

To assess the potential of [Cu(Dp44mT)(OAc)], [Cu(Dp44mT)$_2$], [Cu(Ap44mT)(OAc)], and [Cu(Ap44mT)$_2$] or their free ligands to generate potentially cytotoxic ROS, in vitro studies were initiated simulating physiological (reducing) conditions (i.e., pH 7.4 and the presence of cysteine) in an oxygen-containing environment.[38] These experiments examined the degree of oxidation of nonfluorescent 2′,7′-dichlorodihydrofluorescein (H_2DCF) to fluorescent dichlorofluorescein

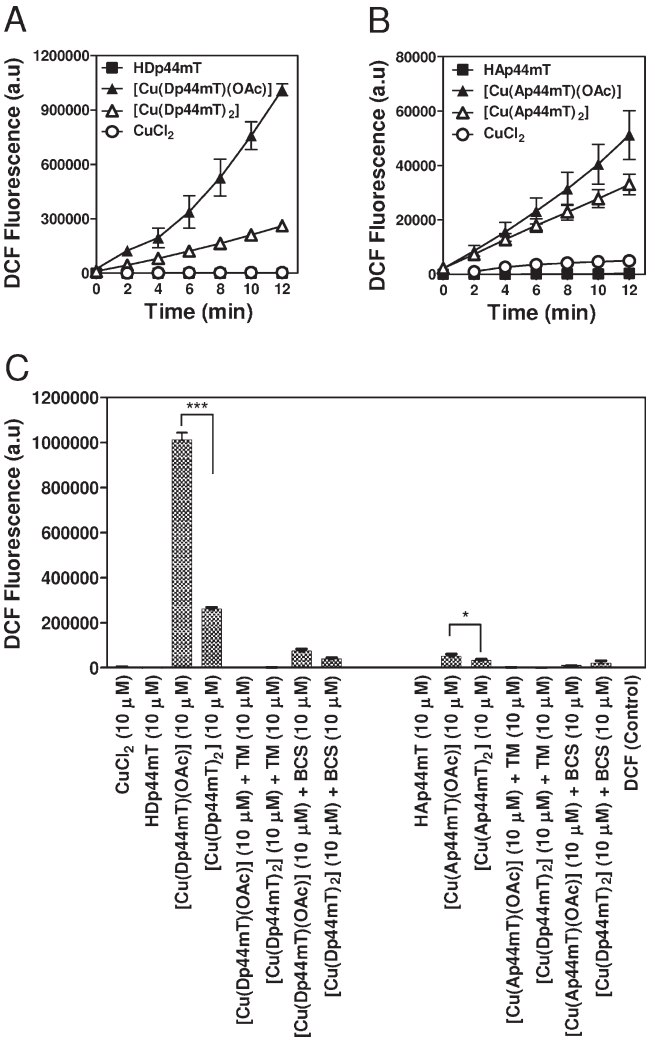

Figure 8. Redox activity of [Cu(Dp44mT)(OAc)], [Cu(Dp44mT)$_2$], [Cu(Ap44mT)(OAc)], and [Cu(Ap44mT)$_2$], as demonstrated by the oxidation of nonfluorescent H_2DCF to fluorescent DCF in vitro under physiologically relevant conditions (i.e., pH 7.4, reducing conditions): kinetic curves of (A) Cu-Dp44mT complexes (10 μM) and (B) Cu-Ap44mT complexes (10 μM) up to an incubation time of 12 min/20 °C; (C) redox activity of the Cu complexes of **H**Dp44mT and **H**Ap44mT (10 μM) in the presence of the Cu chelator, tetrathiomolybdate (TM, 10 μM) or bathocuproine disulphonate (BCS, 10 μM), after a 12 min incubation at 20 °C. Results are the mean ± SD (n = 6): (*) $p < 0.05$, (***) $p < 0.001$.

(DCF) actuated by hydroxyl radicals generated catalytically.[19,39] The Cu^{II} complexes of **H**Dp44mT ([Cu(Dp44mT)(OAc)], Figure 8A) and **H**Ap44mT (Cu(Ap44mT)(OAc), Figure 8B) at a molar ratio of 1:1 demonstrated significantly ($p < 0.01$) more activity between 10 and 12 min of incubation than the Cu complexes at a 2:1 ligand to Cu molar ratio. However, there was a more pronounced difference in the redox activity of the **H**Dp44mT 1:1 ligand/Cu complex compared to its respective 2:1 complex (Figure 8A) relative to the redox activity of the analogous **H**Ap44mT Cu complexes (Figure 8B). In addition, all Cu complexes were significantly ($p < 0.001$) more active at oxidizing H_2DCF than $CuCl_2$ and the ligand alone.

As shown in Figure 8C, after a 12 min incubation, the [Cu(Dp44mT)(OAc)] complex was the most efficient at oxidizing H_2DCF, followed in decreasing order of activity by [Cu(Dp44mT)$_2$], [Cu(Ap44mT)(OAc)], and [Cu(Ap44mT)$_2$]. It is notable from Figure 8C that [Cu(Dp44mT)(OAc)] was 3.9-fold more effective than [Cu(Dp44mT)$_2$] at oxidizing nonfluorescent H_2DCF to fluorescent DCF, while [Cu(Ap44mT)(OAc)] showed 1.6-fold greater activity than [Cu(Ap44mT)$_2$]. A far greater difference in activity was found when comparing the analogous Cu complexes of **H**Dp44mT and **H**Ap44mT. In this case, the oxidation of nonfluorescent H_2DCF to fluorescent DCF was 19.8-fold greater ($p < 0.001$) by [Cu(Dp44mT)(OAc)] relative to [Cu(Ap44mT)(OAc)] and 7.9-fold greater ($p < 0.001$) by [Cu(Dp44mT)$_2$] than [Cu(Ap44mT)$_2$] (Figure 8C). Addition of the clinically used Cu chelator, tetrathiomolybdate (TM),[12] to each Cu thiosemicarbazone complex totally suppressed all catalytic oxidation activity, while another Cu chelator, bathocuproine disulfonate (BCS),[40] inhibited the redox activity of the Cu-Dp44mT complexes by 85−93% and the Cu-Ap44mT complexes by 37−80% (Figure 8C). These results were consistent with the ability of TM and BCS to sequester Cu from the thiosemicarbazone complexes and clearly link the redox cycling of the Cu complexes with H_2DCF oxidation. The well-known hydroxyl radical scavenger DMSO (10% v/v)[41] also suppressed H_2DCF oxidation by all the Cu complexes to 5−35% of that observed in aqueous solution alone (data not shown). These latter data support the suggestion that the oxidizing species in this case was $OH^{\bullet}$.

Increased Intracellular ROS Damage by Cu-Dp44mT and Cu-Ap44mT Complexes. To confirm the pronounced redox activity of the Cu-Dp44mT and Cu-Ap44mT complexes shown in vitro above, the ability of this complex to catalyze the production of intracellular ROS in SK-N-MC cells was assessed using the fluorescent DCF probe and flow cytometry (Figure 9A, B). This method is well established for assessing intracellular redox stress.[19,39] In these studies, the cells were incubated with H_2DCF-DA for 30 min at 37 °C, washed, and then reincubated with control media or the agents for 30 min at 37 °C and flow cytometry was performed.

Incubation of cells with the 1:1 or 1:2 copper complexes of either **H**Dp44mT (Figure 9A) or **H**Ap44mT (Figure 9B) led to an increase of DCF fluorescence intensity resulting in the peak being shifted to the right relative to the control cells. This reflects the increased oxidative damage to these cell populations by the Cu complexes. Quantification of the results in parts A and B of Figure 9 demonstrated that [Cu(Dp44mT)(OAc)] caused a significant ($p < 0.001$) increase in H_2DCF oxidation to 750 ± 20% of control cells after a 30 min incubation (Figure 9C). The [Cu(Dp44mT)-(OAc)] complex was found to be only 14−25% more effective than [Cu(Dp44mT)$_2$], [Cu(Ap44mT)(OAc)], and [Cu(Ap44mT)$_2$] in inducing intracellular ROS. However, Cu/ligand complexes of 1:1 ratio for both **H**Dp44mT and **H**Ap44mT were found to be significantly ($p < 0.01$) more active than the Cu/ligand complexes at a 1:2 ratio (Figure 9C). No significant increase in H_2DCF oxidation could be observed with the same concentration of **H**Dp44mT, **H**Ap44mT or Cu^{II} alone (5 μM) over this relatively short incubation period (Figure 9C). The latter results for **H**Dp44mT are consistent with previous studies over brief incubations (2 h) where little H_2DCF oxidation was observed but in contrast to longer incubations (48 h) where a marked and significant increase in oxidation was found.[19]

The findings above using cells (Figure 9) were somewhat similar to the in vitro catalytic oxidation results with

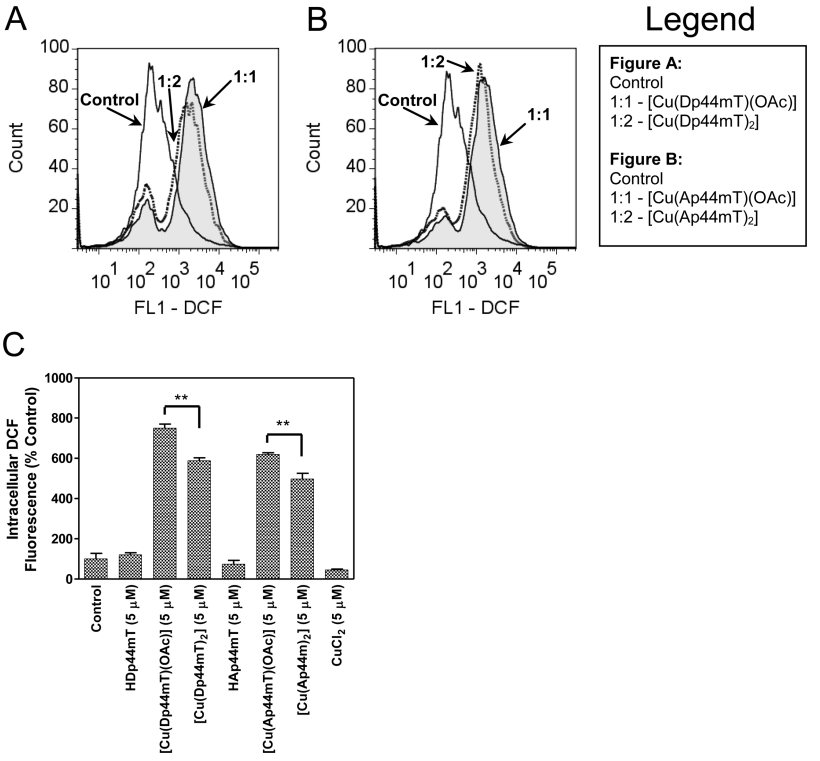

Figure 9. Intracellular production of reactive oxygen species by Cu complexes of **H**Dp44mT and **H**Ap44mT (5 μM) following a 30 min incubation. This was determined by flow cytotometric quantification of the fluorescent DCF probe in SK-N-MC neuroepithelioma cells: (A) control cells (solid line) or cells incubated with [Cu(Dp44mT)(OAc)] (tinted area) or [Cu(Dp44mT)$_2$] (dashed line) for 30 min/37 °C; (B) control cells (solid line) or cells treated with [Cu(Ap44mT)(OAc)] (tinted area) or [Cu(Ap44mT)$_2$](dashed line) for 30 min/37 °C; (C) quantification of the flow cytometric results in (A) and (B) showing the percentage of cells with increased intracellular DCF oxidation compared to control cells. Results are the mean ± SD (n = 6): (**) $p < 0.01$.

H_2DCF/DCF (Figure 8), where the 1:1 Cu/ligand complexes showed the greatest activity in inducing oxidative stress. Importantly, the fact that the intracellular levels of ROS were increased by incubation with these Cu complexes demonstrates that they are able to permeate cell membranes.

Effect of Cu-Dp44mT and Cu-Ap44mT Complexes on Cellular GSH and GSSG Levels. Glutathione (GSH) is a major and well-studied antioxidant, and the GSH/GSSG ratio reflects the cellular redox state.[42] To examine the intracellular redox activity of [Cu(Dp44mT)(OAc)], [Cu(Dp44mT)$_2$], [Cu(Ap44mT)(OAc)], [Cu(Ap44mT)$_2$], and their metal-free ligands, levels of GSH relative to GSSG (oxidized GSH) were assessed after incubation of SK-N-MC cells with these agents and the result was expressed as a GSH/GSSG ratio (Figure 10).

Incubation of cells for 2 h with **H**Ap44mT led to a slight but significant increase in the GSH/GSSG ratio, while a significant ($p < 0.05$) 26% decrease in the ratio was observed after incubation with **H**Dp44mT (Figure 10A). However, after a 24 h incubation, both ligands significantly ($p < 0.01$) lowered the GSH/GSSG ratio by 43% (Figure 10B). The 1:1 ligand to Cu complexes of **H**Dp44mT ([Cu(Dp44mT)(OAc)]) and **H**Ap44mT ([Cu(Ap44mT)(OAc)]) were significantly ($p < 0.01-0.001$) more effective at reducing the GSH/GSSG ratio in SK-N-MC cells than the ligand alone after a 2 h (Figure 10A) or 24 h (Figure 10B) incubation.

The most active agent was [Cu(Dp44mT)(OAc)], which decreased the GSH/GSSG ratio by 100% relative to the control after a 24 h incubation (Figure 10B). The [Cu(Ap44mT)(OAc)] and [Cu(Ap44mT)$_2$] complexes reduced the GSH/GSSG ratio by 90% and 76%, respectively, after 24 h (Figure 10B). These results were similar to the in vitro and intracellular catalytic oxidation results with H_2DCF/DCF (Figures 8 and 9) which indicated that the 1:1 Cu/ligands complexes showed the greatest activity in inducing oxidative stress and lowering the GSH/GSSG ratio. Furthermore, from the assessment of GSH/GSSG ratios, the Cu-Dp44mT complexes caused more oxidative stress to SK-N-MC cells than the Cu-Ap44mT complexes (Figure 10).

Antiproliferative Activity against Tumor Cells: Cu Complexes of HDp44mT and HAp44mT. Many series of chelators have been examined for their effects on cellular proliferation.[43−45] Previous studies have illustrated that complexation of chelators with metal ions can result in marked changes in biological activity.[46] To determine the effect of complexation on the antiproliferative efficacy of **H**Dp44mT and **H**Ap44mT with Cu, complexes of the ligand and Cu in a 1:1 or 1:2 molar ratio were examined using SK-N-MC neuroepithelioma cells (Figure 11).

After a 24 h incubation, this study identified that the antiproliferative activity of **H**Dp44mT (IC_{50} = 0.53 ± 0.16 μM, Figure 11A) was similar to that observed with **H**Ap44mT (IC_{50} = 0.29 ± 0.02 μM, Figure 11B). In comparison with their free ligands, the Cu complexes of **H**Dp44mT and **H**Ap44mT demonstrated significantly ($p < 0.05$) increased antiproliferative activity after a 24 h incubation, while no pronounced antiproliferative effect was observed with $CuCl_2$ alone (Figure 11A,B). After a 72 h incubation, the effects of the ligands and their Cu complexes were more marked than that found after 24 h (Figure 11C,D). Furthermore, IC_{90} values (the concentration that inhibits proliferation by 90%) after a 24 and 72 h incubation revealed that the complexes of ligand to Cu at a 1:1 molar ratio were significantly

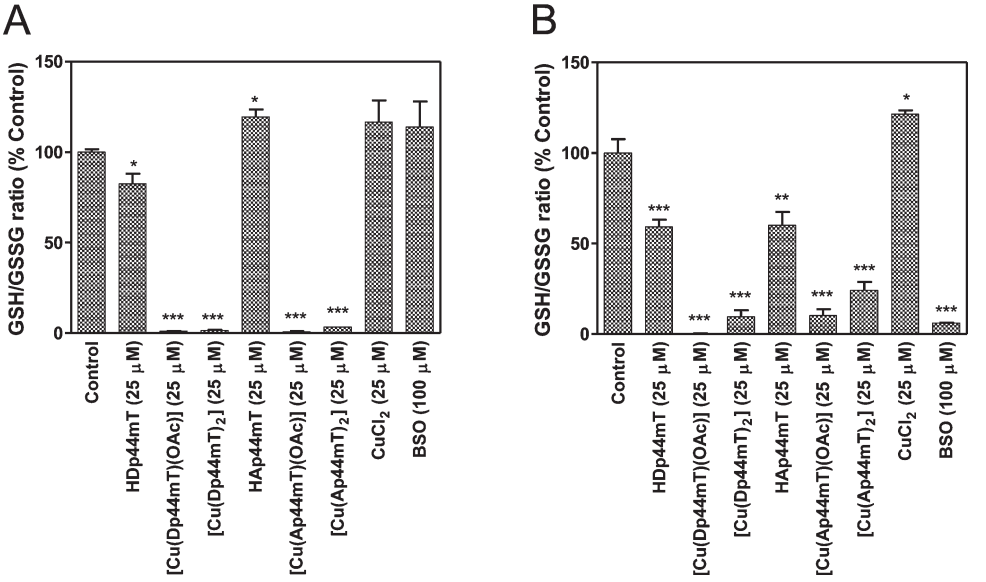

Figure 10. Incubation for either (A) 2 h or (B) 24 h at 37 °C with [Cu(Dp44mT)(OAc)], [Cu(Dp44mT)$_2$], [Cu(Ap44mT)(OAc)], [Cu(Ap44mT)$_2$], **H**Dp44mT, **H**Ap44mT (25 μM), or the GSH-synthesis inhibitor buthionine sulfoximine (BSO, 100 μM) decreases the GSH/GSSG ratio in cultured SK-N-MC neuroepithelioma cells. Results are the mean ± SD (n = 6): (*) $p < 0.05$, (**) $p < 0.01$, (***) $p < 0.001$.

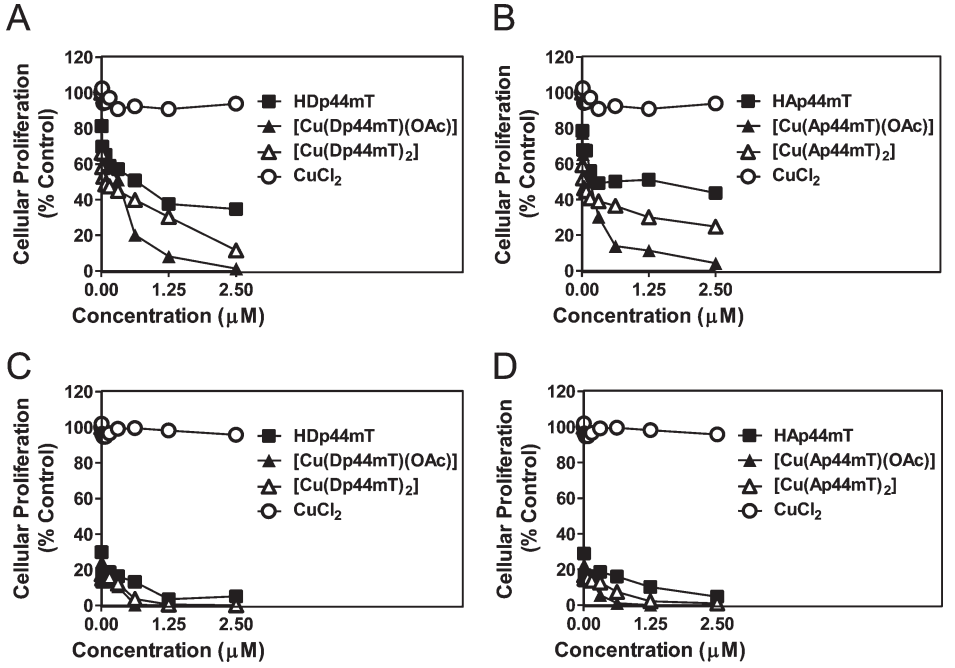

Figure 11. Rapid decrease in the growth of SK-N-MC cells can be observed with [Cu(Dp44mT)(OAc)], [Cu(Dp44mT)$_2$], [Cu(Ap44mT)-(OAc)], or [Cu(Ap44mT)$_2$] compared to the ligands **H**A44mT and **H**Dp44mT alone. Cellular proliferation was determined by the MTT assay after incubations of (A, B) 24 h or (C, D) 72 h at 37 °C. Results are the mean ± SD of at least n = 3 experiments.

($p < 0.01-0.001$) more active than the respective complexes at a 2:1 molar ratio (Table 3).

Assessing the IC_{90} values, the complexes derived from **H**Dp44mT were more effective than those derived from **H**Ap44mT at inhibiting proliferation. In fact, the [Cu-(Dp44mT)(OAc)] and [Cu(Dp44mT)$_2$] complexes (IC_{90} of 1.18 ± 0.04 and 3.05 ± 0.06 μM, respectively) caused significantly ($p < 0.01$) more inhibition of proliferation of SK-N-MC cells than the [Cu(Ap44mT)(OAc)] and [Cu(Ap44mT)$_2$] complexes (IC_{90} of 1.49 ± 0.08 and >5 μM, respectively) after a 24 h incubation (Table 3). This is consistent with the systematically higher redox potentials of the Cu-Dp44mT complexes due to the electron-withdrawing effect of the noncoordinating 2-pyridyl ring in comparison with the electron-donating methyl group in the acetylpyridine analogues. In this case, the [Cu(Dp44mT)(OAc)] complex, or its solvated analogue, exhibits a redox potential that is high enough to oxidize cellular reductants such as GSH while being sufficiently low so that reaction of the Cu^I complex with oxidants such as H_2O_2 or O_2 is fast enough to result in significant quantities of cytotoxic ROS. In other words, there is an optimal window of redox activity that favors redox cycling. Similar findings have emerged from our previous studies with Fe complexes of these ligands where the redox potential of the Fe complex has been strongly correlated with antiproliferative activity.[2,22,23]

Table 3. IC_{50} and IC_{90} for Copper Complexes of HDp44mT and HAp44mT in SK-N-MC Neuroepithelioma Cells after a 24 or 72 h Incubation[a]

	24 h		72 h	
	IC_{50} (μM)	IC_{90} (μM)	IC_{50} (μM)	IC_{90} (μM)
HDp44mT	0.53 ± 0.16	>5	<0.01	0.76 ± 0.08
[Cu(Dp44mT)(OAc)]	0.23 ± 0.11	1.18 ± 0.04	<0.01	0.33 ± 0.01
[Cu(Dp44mT)$_2$]	0.11 ± 0.05	3.05 ± 0.62	<0.01	0.39 ± 0.01
HAp44mT	0.29 ± 0.02	>5	<0.01	1.46 ± 0.24
[Cu(Ap44mT)(OAc)]	0.12 ± 0.04	1.49 ± 0.08	<0.01	0.22 ± 0.02
[Cu(Ap44mT)$_2$]	0.05 ± 0.03	>5	<0.01	0.44 ± 0.03
$CuCl_2$	>5	>5	>5	>5

[a] Results are the mean ± SD (three experiments).

It is notable that precomplexation with Cu increases antiproliferative activity compared to both **H**Dp44mT and **H**Ap44mT alone (Figure 11A,B). These results can probably be explained by the fact that the Cu complexes are cytotoxic because of their redox activity (Figures 8 and 9). Another factor may be that relative to the ligands, the Cu complexes are more able to cross the cell membrane because of their predicted greater lipophilicity.

Considering the role of Fenton chemistry in the mechanism of action of these compounds, how can these compounds be selective against cancer cells? We already know that **H**Dp44mT and many of its analogues show selective antitumor activity in vitro in cell culture when tested against normal and neoplastic cells and also in vivo in mouse studies against a murine tumor and a variety of human tumor xenografts.[19,21,22,47] The reason for the selectivity may be, at least in part, due to the fact that tumor cells show differences in both Fe and Cu metabolism relative to normal tissues,[12] but other factors may also be important to consider, such as membrane permeability, etc.

Conclusions

In summary, thiosemicarbazones are an important group of Fe chelators that show potent and selective antitumor activity.[2,3,29,30,48,49] Our studies indicate that their ability to also bind Cu is also linked to their antiproliferative efficacy. The current investigation highlights the importance of Cu chelation in understanding the overall mechanism of antitumor activity for two of the most active thiosemicarbazones developed in our laboratories, namely, **H**Dp44mT and **H**Ap44mT.[2,19,23] Indeed, it is important to note that both Cu and Fe chelation by this class of ligands can lead to redox active complexes and that the formation of both is probably important for the cytotoxicity of these compounds.[2,19,23]

An interesting result from our characterization of the Cu^{II} coordination chemistry of these compounds was the fact that both the 1:1 and 1:2 Cu/ligand complexes could be isolated and that the 1:2 complexes dissociate to give significant amounts of the 1:1 analogue. In fact, the higher biological activity of the 1:1 complexes suggests that these may be the active species in cells, while the 1:2 complexes could be precursors to the 1:1 complex formed by partial dissociation.

We have also demonstrated the significance of substituents on the carbonyl group of the parent ketone (C6 in Figures 2 and 3) and the consequential redox stress to cells. The inductive effects of groups at this position were observed to influence the $Cu^{II/I}$ redox potentials because of their proximity to the metal center. **H**Dp44mT containing an electron-withdrawing substituent exhibited higher $Cu^{II/I}$ redox potentials than the Cu complexes of **H**Ap44mT. However, Cu-Ap44mT complexes did maintain the ability to oxidize H_2DCF and induce intracellular stress and exhibited generally lower antiproliferative activity relative to the Cu-Dp44mT complexes.

Considering the above conclusion, another important observation from this study was the increased antitumor activity of the Cu-Dp44mT and Cu-Ap44mT complexes relative to the ligand alone or their Fe complexes.[23] These findings highlight the contribution of Cu chelation to the marked cytotoxicity induced by these thiosemicarbazones and should provide useful clues in the design of even more effective agents for cancer treatment.

Experimental Procedures

Chemical Studies. Physical Methods. Cyclic voltammetry was performed using a BAS100B/W potentiostat. A glassy carbon working electrode, an aqueous Ag/AgCl reference electrode, and a Pt wire auxiliary electrode were used. All complexes were at ~1 mM in MeCN/H_2O (7:3 v/v). This solvent combination was used to ensure the solubility of all compounds. The supporting electrolyte was Et_4NClO_4 (0.1 M), and the solutions were purged with nitrogen prior to measurement. All potentials are cited versus the normal hydrogen electrode (NHE) by addition of 196 mV to the potentials measured relative to the Ag/AgCl reference. Electron paramagnetic resonance (EPR) spectra were measured on a Bruker ER200 instrument at X-band frequency (~9.3 GHz) in 1 mM DMF frozen solutions at 77 K. Spectra were simulated with the program EPR50F.[50] All simulated spectra and their spin Hamiltonian parameters appear in the Supporting Information. The purity of synthesized compounds were analyzed via combustion analysis and were found to be ≥95% pure.

Syntheses. The ligands **H**Dp44mT[2] and **H**Ap44mT[23] and the complex [Cu(Dp44mT)$_2$][29] were synthesized according to reported procedures.

[Cu(Dp44mT)(OAc)]. **H**Dp44mT (0.285 g, 1 mmol) was dissolved in DMF (7 mL) with gentle heating and stirring. A solution of $Cu(OAc)_2 \cdot H_2O$ (0.20 g, 1 mmol) in water (7 mL) was added dropwise with stirring, and the ligand solution immediately turned dark brown. Fine olive-green-brown crystals formed on standing, which were filtered off, washed with EtOH (5 mL) and then diethyl ether (5 mL), and dried in a vacuum desiccator overnight (yield 0.18 g, 44%). Anal. Calcd for $C_{16}H_{17}CuN_5SO_2$: C 38.0%; H 3.8%; N 17.7%. Found: C 37.7%; H 3.7%; N 17.6%. UV/vis (DMSO) λ_{max} 435 nm (ε 16 560 $M^{-1}cm^{-1}$). EPR (DMF, 77K) $g_x = g_y = 2.040$, $g_z = 2.193$; hyperfine coupling constants $A_{Cu,x} = A_{Cu,y} = 20.0$ G, $A_{Cu,z} = 183.0$ G; superhyperfine coupling constants $A_{N,x} = A_{N,y} = A_{N,z} = 16.0$ G.

[Cu(Ap44mT)(OAc)]. The same procedure was followed as for preparing [Cu(Dp44mT)(OAc)], except **H**Ap44mT was substituted as the ligand, affording dark greenish-brown needles suitable for X-ray work (yield 0.14 g, 49.3%). Anal. Calcd for $C_{12}H_{16}CuN_4SO_2$: C 41.9%; H 4.7%; N 16.3%. Found: C 42.1%; H 4.7%; N 16.4%. UV/vis (DMSO) λ 418 nm ε (14 880 $M^{-1}cm^{-1}$). EPR (DMF, 77K) $g_x = g_y = 2.050$, $g_z = 2.183$; hyperfine coupling constants $A_{Cu,x} = A_{Cu,y} = 20.0$ G, $A_{Cu,z} = 183.0$ G; superhyperfine coupling constants $A_{N,x} = A_{N,y} = A_{N,z} = 16.0$ G.

[Cu(Ap44mT)$_2$]. **H**Ap44mT (0.22 g, 1 mmol) was suspended in EtOH (15 mL). Triethylamine (0.37 g, 2 mmol) was added, and the mixture was warmed gently to dissolve the ligand. A solution of $Cu(ClO_4)_2 \cdot 6H_2O$ (0.185 g, 0.5 mmol) in EtOH (2 mL) was added dropwise to the ligand solution with stirring. The mixture was refluxed gently for 30 min and then allowed to cool at room temperature. On standing, the dark green crystalline product was filtered off and washed with EtOH (2 × 5 mL), then dried in a vacuum desiccator (yield = 0.19 g,

74%). Anal. Calcd for $CuC_{20}H_{26}N_8S_2$: C 47.5%; H 5.2%; N 22.1%. Found: C 47.0%; H 5.3%; N 22.1%. UV/vis (DMSO) λ_{max} nm (ε L mol^{-1} cm^{-1}): 403 (24 900). EPR (DMF, 77K) $g_x = g_y = 2.080$, $g_z = 2.162$; hyperfine coupling constants $A_{Cu,x} = A_{Cu,y} = 20.0$ G; $A_{Cu,z} = 159.0$ G.

Crystallography. Crystallographic data were acquired at 293 K on an Oxford Diffraction Gemini CCD diffractometer employing graphite-monochromated Mo Kα radiation (0.710 73 Å) and operating within the range $2 < 2\theta < 50$ Å. Data reduction and empirical absorption corrections (multiscan) were performed with Oxford Diffraction CrysAlisPro software. Structures were solved by direct methods with SHELXS and refined by full-matrix least-squares analysis with SHELXL-97.[51] All non-H atoms were refined with anisotropic thermal parameters. Molecular structure diagrams were produced with ORTEP3.[52] The data in CIF format have been deposited at the Cambridge Crystallographic Data Centre (CCDC 775627 and 775628). Crystal data and selected bond lengths appear in Table 1 and 2, respectively.

Biological Studies. Cell Culture. Chelators were dissolved in DMSO as 10 mM stock solutions and diluted in medium containing 10% fetal calf serum (Commonwealth Serum Laboratories, Melbourne, Australia) so that the final [DMSO] < 0.5% (v/v). At this DMSO concentration there was no effect on proliferation.[53] The SK-N-MC neuroepithelioma cell line (American Type Culture Collection, Manassas, VA) was grown as previously described[53] at 37 °C in a humidified atmosphere of 5% CO_2/95% air in an incubator (Forma Scientific, Marietta, OH). This cell type was used as its response to chelators, and their metal complexes have been well characterized in our previous studies.[2,23,53,54]

DCF Assay: Estimation of Fenton-Type Reactions. In order to assay if Fenton-type reactions are induced by the Cu complexes of **H**Dp44mT and **H**Ap44mT under physiological conditions (pH 7.4), experiments with DCF were done in vitro using standard techniques.[39] Briefly, as a positive control, Cu^{II} at 10 μM was reduced to Cu^{I} using cysteine (100 μM) in 20 mM HEPES buffer (pH 7.4). Hydrogen peroxide (100 μM) was then added to initiate hydroxyl radical ($OH^{\bullet}$) generation. The latter oxidizes nonfluorescent H_2DCF (5 μM) to fluorescent DCF. H_2DCF was obtained by hydrolyzing its acetate ester in vitro (H_2DCF-DA).[55] The hydroxyl radical scavenger DMSO (10%) was used to confirm hydroxyl radical generation, while the Cu chelators TM (10 μM) and BCS (10 μM) were used to demonstrate the involvement of Cu in the reaction. Fluorescence was measured using a FL600 microplate reader (Victor 2, Wallac, Turku, Finland) at $\lambda_{ex} = 485$ nm and $\lambda_{em} = 530$ nm.

Intracellular ROS Measurements. Intracellular ROS generation was measured using H_2DCF-DA.[19,39] H_2DCF-DA is hydrolyzed by intracellular esterases to H_2DCF, which leads to it becoming trapped within the cytosol. Cellular oxidants localized to the cytosol oxidize nonfluorescent H_2DCF to the fluorescent product DCF.[19,39] SK-N-MC cells were incubated with 30 μM H_2DCF-DA for 30 min at 37 °C and then washed twice with ice-cold PBS. The cells were then treated with either **H**Dp44mT (5 μM), **H**Ap44mT (5 μM), Cu(II) (5 μM), or the Cu complexes of **H**Dp44mT or **H**Ap44mT (5 μM) for 30 min at 37 °C. Cells were collected for flow cytometric assessment. Intracellular ROS was detected as an increase in green cytosolic DCF fluorescence with a FACS Canto flow cytometer (Becton Dickinson, Lincoln Park, NJ), and 10 000 events were acquired for every sample. Data analysis was performed using FlowJo software, version 7.5.5 (Tree Star Inc., Ashland, OR).

Intracellular GSH/GSSG Assay. The GSH/GSSG ratio reflects the cellular redox state,[56] and this was assessed using an assay kit (Calbiochem, La Jolla, CA) based on the enzymatic recycling method using glutathione reductase.[57] SK-N-MC cells were seeded in 10 cm tissue culture plates at 2.5×10^6 cells/plate and incubated overnight before treatment. Cells were treated for 2 or 24 h at 37 °C with [Cu(Dp44mT)(OAc)], [Cu(Dp44mT)$_2$], [Cu(Ap44mT)(OAc)], [Cu(Ap44mT)$_2$], **H**Dp44mT, **H**Ap44mT, $CuCl_2$ (25 μM), or the GSH-synthesis inhibitor buthionine sulfoximine (BSO)[58] (100 μM).

Cells were detached with EDTA (1 mM in calcium/magnesium-free PBS) and prepared according to the instructions obtained with the GSH/GSSG ratio assay kit (Calbiochem, CA). Briefly, for the GSSG sample, the thiol-scavenging reagent 1-methy-2-vinylpyridinium trifluoromethanesulfonate was immediately mixed with the cell suspension to eliminate GSH. Cells were frozen and thawed and then extracted with metaphosphoric acid. The cell lysates were added to GSSG or GSH assay buffers, respectively. Samples were mixed sequentially with the chromogen, 5,5′-dithiobis-2-nitrobenzoic acid, glutathione reductase, and NADPH. Absorbance at 405 nm was recorded for 3 min at room temperature (20 °C), and the reaction rate was determined. A standard curve was constructed using a known quantity of GSH (Sigma-Aldrich). The GSH and GSSG concentrations were calculated by linear regression against the standard curve. The GSH/GSSG ratio was obtained from the equation [ratio = (GSH − 2GSSG)/GSSG]. The results were expressed as a percentage of the control.

Preparation of Diferric Transferrin. Human transferrin (Tf, Sigma) was saturated with Fe to produce diferric Tf, as previously described.[10,11] Unbound Fe was removed by exhaustive vacuum dialysis against a large excess of 0.15 M NaCl buffered with 1.4% $NaHCO_3$ by standard methods.[10,11] The diferric Tf was added in all cellular proliferation experiments (see below) to simulate physiological conditions where this protein donates Fe to cells.[7]

Effect of the Chelators and Complexes on Cellular Proliferation. The effects of the chelators and complexes on cellular proliferation were determined by the MTT [1-(4,5-dimethylthiazol-2-yl)-2,5-diphenyltetrazolium] assay using standard techniques.[30,53] The SK-N-MC cell line was seeded in 96-well microtiter plates at 1.0×10^4 cells/well in medium containing human diferric Tf (1.25 μM) and chelators or complexes at a range of concentrations (0−2.5 μM). Control samples contained medium with diferric Tf (1.25 μM) without the ligands. The cells were incubated at 37 °C in a humidified atmosphere containing 5% CO_2 and 95% air for 24 or 72 h. After this incubation, 10 μL of MTT (5 mg/mL) was added to each well and the incubation continued at 37 °C for 2 h. After solubilization of the cells with 100 μL of 10% SDS−50% isobutanol in 10 mM HCl, the plates were read at 570 nm using a scanning multiwell spectrophotometer. The results, which are the mean values of three experiments, are expressed as a percentage of the control. The inhibitory concentration (IC_{50} and IC_{90}) was defined as the concentration of chelator or complex necessary to reduce the absorbance to 50% and 90% of the untreated control, respectively. By use of this method, absorbance was shown to be directly proportional to cell counts, as shown previously.[53]

Statistical Analysis. Experimental data were compared using Student's t test. Results were expressed as the mean or the mean ± SD (number of experiments) and considered to be statistically significant when $p < 0.05$. All experiments were repeated three to six times.

Acknowledgment. D.R.R. and P.V.B. thank the Australian Research Council for Discovery Grant funding and a Project Grant from the National Health and Medical Research Council of Australia (NHMRC). D.R.R. is the grateful recipient of an NHMRC Senior Principal Research Fellowship. D.R.R. and P.J.J. appreciate grant support from the Australian Rotary Health Research Foundation.

Supporting Information Available: Simulated and experimental EPR spectra including spin Hamiltonian parameters. This material is available free of charge via the Internet at http://pubs.acs.org.

References

(1) Bernhardt, P. V.; Caldwell, L. M.; Chaston, T. B.; Chin, P.; Richardson, D. R. Cytotoxic iron chelators: characterization of the structure, solution chemistry and redox activity of ligands and iron complexes of the di-2-pyridyl ketone isonicotinoyl hydrazone (HPKIH) analogues. *J. Biol. Inorg. Chem.* **2003**, *8*, 866–880.

(2) Richardson, D. R.; Sharpe, P. C.; Lovejoy, D. B.; Senaratne, D.; Kalinowski, D. S.; Islam, M.; Bernhardt, P. V. Dipyridyl thiosemicarbazone chelators with potent and selective antitumor activity form iron complexes with redox activity. *J. Med. Chem.* **2006**, *49*, 6510–6521.

(3) Buss, J. L.; Greene, B. T.; Turner, J.; Torti, F. M.; Torti, S. V. Iron chelators in cancer chemotherapy. *Curr. Top. Med. Chem.* **2004**, *4*, 1623–1635.

(4) Kalinowski, D. S.; Richardson, D. R. Future of toxicology—iron chelators and differing modes of action and toxicity: the changing face of iron chelation therapy. *Chem. Res .Toxicol.* **2007**, *20*, 715–720.

(5) Rakba, N.; Loyer, P.; Gilot, D.; Delcros, J. G.; Glaise, D.; Baret, P.; Pierre, J. L.; Brissot, P.; Lescoat, G. Antiproliferative and apoptotic effects of O-Trensox, a new synthetic iron chelator, on differentiated human hepatoma cell lines. *Carcinogenesis* **2000**, *21*, 943–951.

(6) Torti, S. V.; Torti, F. M.; Whitman, S. P.; Brechbiel, M. W.; Park, G.; Planalp, R. P. Tumor cell cytotoxicity of a novel metal chelator. *Blood* **1998**, *92*, 1384–1389.

(7) Yu, Y.; Kalinowski, D. S.; Kovacevic, Z.; Siafakas, A. R.; Jansson, P. J.; Stefani, C.; Lovejoy, D. B.; Sharpe, P. C.; Bernhardt, P. V.; Richardson, D. R. Thiosemicarbazones from the old to new: iron chelators that are more than just ribonucleotide reductase inhibitors. *J. Med. Chem.* **2009**, *52*, 5271–5294.

(8) Kalinowski, D. S.; Richardson, D. R. The evolution of iron chelators for the treatment of iron overload disease and cancer. *Pharmacol. Rev.* **2005**, *57*, 547–583.

(9) Trinder, D.; Zak, O.; Aisen, P. Transferrin receptor-independent uptake of differic transferrin by human hepatoma cells with antisense inhibition of receptor expression. *Hepatology* **1996**, *23*, 1512–1520.

(10) Richardson, D. R.; Baker, E. The uptake of iron and transferrin by the human malignant melanoma cell. *Biochim. Biophys. Acta* **1990**, *1053*, 1–12.

(11) Richardson, D.; Baker, E. Two mechanisms of iron uptake from transferrin by melanoma cells. The effect of desferrioxamine and ferric ammonium citrate. *J. Biol. Chem.* **1992**, *267*, 13972–13979.

(12) Yu, Y.; Wong, J.; Lovejoy, D. B.; Kalinowski, D. S.; Richardson, D. R. Chelators at the cancer coalface: desferrioxamine to Triapine and beyond. *Clin. Cancer Res.* **2006**, *12*, 6876–6883.

(13) Morgan, E. H. Transferrin biochemistry, physiology and clinical significance. *Mol. Aspects Med.* **1981**, 1–123.

(14) Larrick, J. W.; Cresswell, P. Modulation of cell surface iron transferrin receptors by cellular density and state of activation. *J. Supramol. Struct.* **1979**, *11*, 579–586.

(15) Daniel, K. G.; Gupta, P.; Harbach, R. H.; Guida, W. C.; Dou, Q. P. Organic copper complexes as a new class of proteasome inhibitors and apoptosis inducers in human cancer cells. *Biochem. Pharmacol.* **2004**, *67*, 1139–1151.

(16) Gupte, A.; Mumper, R. J. Elevated copper and oxidative stress in cancer cells as a target for cancer treatment. *Cancer Treat. Rev.* **2009**, *35*, 32–46.

(17) Xie, H.; Kang, Y. J. Role of copper in angiogenesis and its medicinal implications. *Curr. Med. Chem.* **2009**, *16*, 1304–1314.

(18) Hassouneh, B.; Islam, M.; Nagel, T.; Pan, Q.; Merajver, S. D.; Teknos, T. N. Tetrathiomolybdate promotes tumor necrosis and prevents distant metastases by suppressing angiogenesis in head and neck cancer. *Mol. Cancer Ther.* **2007**, *6*, 1039–1045.

(19) Yuan, J.; Lovejoy, D. B.; Richardson, D. R. Novel di-2-pyridyl-derived iron chelators with marked and selective antitumor activity: in vitro and in vivo assessment. *Blood* **2004**, *104*, 1450–1458.

(20) Lowndes, S. A.; Adams, A.; Timms, A.; Fisher, N.; Smythe, J.; Watt, S. M.; Joel, S.; Donate, F.; Hayward, C.; Reich, S.; Middleton, M.; Mazar, A.; Harris, A. L. Phase I study of copper-binding agent ATN-224 in patients with advanced solid tumors. *Clin. Cancer Res.* **2008**, *14*, 7526–7534.

(21) Whitnall, M.; Howard, J.; Ponka, P.; Richardson, D. R. A class of iron chelators with a wide spectrum of potent anti-tumor activity that overcome resistance to chemotherapeutics. *Proc. Natl. Acad. Sci. U.S.A.* **2006**, *103*, 14901–14906.

(22) Kalinowski, D. S.; Yu, Y.; Sharpe, P. C.; Islam, M.; Liao, Y. T.; Lovejoy, D. B.; Kumar, N.; Bernhardt, P. V.; Richardson, D. R. Design, synthesis, and characterization of novel iron chelators: structure−activity relationships of the 2-benzoylpyridine thiosemicarbazone series and their 3-nitrobenzoyl analogues as potent antitumor agents. *J. Med. Chem.* **2007**, *50*, 3716–3729.

(23) Richardson, D. R.; Kalinowski, D. S.; Richardson, V.; Sharpe, P. C.; Lovejoy, D. B.; Islam, M.; Bernhardt, P. V. 2-Acetylpyridine thiosemicarbazones are potent iron chelators and antiproliferative agents: redox activity, iron complexation and characterization of their antitumor activity. *J. Med. Chem.* **2009**, *52*, 1459–1470.

(24) Liu, Z. D.; Hider, R. C. Design of iron chelators with therapeutic application. *Coord. Chem. Rev.* **2002**, *232*, 151–171.

(25) Barnham, K. J.; Masters, C. L.; Bush, A. I. Neurodegenerative diseases and oxidative stress. *Nat. Rev. Drug Discovery* **2004**, *3*, 205–214.

(26) Marzano, C.; Pellei, M.; Tisato, F.; Santini, C. Copper complexes as anticancer agents. *Anti-Cancer Agents Med. Chem.* **2009**, *9*, 185–211.

(27) Paterson, B. M.; Karas, J. A.; Scanlon, D. B.; White, J. M.; Donnelly, P. S. Versatile new bis(thiosemicarbazone) bifunctional chelators: synthesis, conjugation to bombesin(7−14)-NH2, and copper-64 radiolabeling. *Inorg. Chem.* **2010**, *49*, 1884–1893.

(28) Xiao, Z.; Donnelly, P. S.; Zimmermann, M.; Wedd, A. G. Transfer of copper between bis(thiosemicarbazone) ligands and intracellular copper-binding proteins. Insights into mechanisms of copper uptake and hypoxia selectivity. *Inorg. Chem.* **2008**, *47*, 4338–4347.

(29) Bernhardt, P. V.; Sharpe, P. C.; Islam, M.; Lovejoy, D. B.; Kalinowski, D. S.; Richardson, D. R. Iron chelators of the dipyridylketone thiosemicarbazone class: precomplexation and transmetalation effects on anticancer activity. *J. Med. Chem.* **2009**, *52*, 407–415.

(30) Kalinowski, D. S.; Sharpe, P. C.; Bernhardt, P. V.; Richardson, D. R. Design, synthesis, and characterization of new iron chelators with anti-proliferative activity: structure−activity relationships of novel thiohydrazone analogues. *J. Med. Chem.* **2007**, *50*, 6212–6225.

(31) Hathaway, B. J. A new look at the stereochemistry and electronic properties of complexes of the copper(II) ion. *Struct. Bonding (Berlin)* **1984**, *57*, 55–118.

(32) Halcrow, M. A. Interpreting and controlling the structures of six-coordinate copper(II) centres. When is a compression really a compression? *Dalton Trans.* **2003**, 4375–4384.

(33) Huettermann, J.; Kappl, R. EPR and ENDOR of metalloproteins: copper and iron. *Electron Paramagn. Reson.* **2004**, *19*, 116–173.

(34) Valko, M.; Morris, H.; Cronin, M. T. Metals, toxicity and oxidative stress. *Curr. Med. Chem.* **2005**, *12*, 1161–1208.

(35) Fenton, H. J. H. On a new reaction of tartaric acid. *Chem. News* **1876**, *33*, 190.

(36) Halliwell, B.; Gutteridge, J. M. Biologically relevant metal ion-dependent hydroxyl radical generation. An update. *FEBS Lett.* **1992**, *307*, 108–112.

(37) Wardman, P.; Candeias, L. P. Fenton chemistry: an introduction. *Radiat. Res.* **1996**, *145*, 523–531.

(38) Pisoni, R. L.; Acker, T. L.; Lisowski, K. M.; Lemons, R. M.; Thoene, J. G. A cysteine-specific lysosomal transport system provides a major route for the delivery of thiol to human fibroblast lysosomes: possible role in supporting lysosomal proteolysis. *J. Cell Biol.* **1990**, *110*, 327–335.

(39) Myhre, O.; Andersen, J. M.; Aarnes, H.; Fonnum, F. Evaluation of the probes 2′,7′-dichlorofluorescin diacetate, luminol, and lucigenin as indicators of reactive species formation. *Biochem. Pharmacol.* **2003**, *65*, 1575–1582.

(40) Blair, D.; Diehl, H. Bathophenanthrolinedisulphonic acid and bathocuproinedisulphonic acid, water soluble reagents for iron and copper. *Talanta* **1961**, 163–174.

(41) Santos, N. C.; Figueira-Coelho, J.; Martins-Silva, J.; Saldanha, C. Multidisciplinary utilization of dimethyl sulfoxide: pharmacological, cellular, and molecular aspects. *Biochem. Pharmacol.* **2003**, *65*, 1035–1041.

(42) Meister, A.; Anderson, M. E. Glutathione. *Annu. Rev. Biochem.* **1983**, *52*, 711–760.

(43) Liang, S. X.; Richardson, D. R. The effect of potent iron chelators on the regulation of p53: examination of the expression, localization and DNA-binding activity of p53 and the transactivation of WAF1. *Carcinogenesis* **2003**, *24*, 1601–1614.

(44) Yu, Y.; Kovacevic, Z.; Richardson, D. R. Tuning cell cycle regulation with an iron key. *Cell Cycle* **2007**, *6*, 1982–1994.

(45) Zhao, R.; Planalp, R. P.; Ma, R.; Greene, B. T.; Jones, B. T.; Brechbiel, M. W.; Torti, F. M.; Torti, S. V. Role of zinc and iron chelation in apoptosis mediated by tachpyridine, an anti-cancer iron chelator. *Biochem. Pharmacol.* **2004**, *67*, 1677–1688.

(46) Richardson, D. R. Mobilization of iron from neoplastic cells by some iron chelators is an energy-dependent process. *Biochim. Biophys. Acta* **1997**, *1320*, 45–57.

(47) Noulsri, E.; Richardson, D. R.; Lerdwana, S.; Fucharoen, S.; Yamagishi, T.; Kalinowski, D. S.; Pattanapanyasat, K. Antitumor

activity and mechanism of action of the iron chelator, Dp44mT, against leukemic cells. *Am. J. Hematol.* **2009**, *84*, 170–176.
(48) Kowol, C. R.; Berger, R.; Eichinger, R.; Roller, A.; Jakupec, M. A.; Schmidt, P. P.; Arion, V. B.; Keppler, B. K. Gallium(III) and iron(III) complexes of alpha-N-heterocyclic thiosemicarbazones: synthesis, characterization, cytotoxicity, and interaction with ribonucleotide reductase. *J. Med. Chem.* **2007**, *50*, 1254–1265.
(49) Kowol, C. R.; Eichinger, R.; Jakupec, M. A.; Galanski, M.; Arion, V. B.; Keppler, B. K. Effect of metal ion complexation and chalcogen donor identity on the antiproliferative activity of 2-acetylpyridine *N*,*N*-dimethyl(chalcogen)semicarbazones. *J. Inorg. Biochem.* **2007**, *101*, 1946–1957.
(50) Martinelli, R. A.; Hanson, G. R.; Thompson, J. S.; Holmquist, B.; Pilbrow, J. R.; Auld, D. S.; Vallee, B. L. Characterization of the inhibitor complexes of cobalt carboxypeptidase A by electron paramagnetic resonance spectroscopy. *Biochemistry* **1989**, *28*, 2251–2258.
(51) Sheldrick, G. M. *SHELX97. Programs for Crystal Structure Analysis*, release 97-2; University of Göttingen: Göttingen, Germany, 1998.
(52) Farrugia, L. J. ORTEP-3 for Windows: a version of ORTEP-III with a graphical user interface (GUI). *J. Appl. Crystallogr.* **1997**, *30*, 565.
(53) Richardson, D. R.; Tran, E. H.; Ponka, P. The potential of iron chelators of the pyridoxal isonicotinoyl hydrazone class as effective antiproliferative agents. *Blood* **1995**, *86*, 4295–4306.
(54) Richardson, D. R.; Ponka, P. The iron metabolism of the human neuroblastoma cell. Lack of relationship between the efficacy of iron chelation and the inhibition of DNA synthesis. *J. Lab. Clin. Med.* **1994**, *124*, 660–671.
(55) Mladenka, P.; Kalinowski, D. S.; Haskova, P.; Bobrovova, Z.; Hrdina, R.; Simunek, T.; Nachtigal, P.; Semecky, V.; Vavrova, J.; Holeckova, M.; Palicka, V.; Mazurova, Y.; Jansson, P. J.; Richardson, D. R. The novel iron chelator, 2-pyridylcarboxaldehyde 2-thiophenecarboxyl hydrazone, reduces catecholamine-mediated myocardial toxicity. *Chem. Res. Toxicol.* **2009**, *22*, 208–217.
(56) Meister, A. Glutathione metabolism and its selective modification. *J. Biol. Chem.* **1988**, *263*, 17205–17208.
(57) Griffith, O. W. Determination of glutathione and glutathione disulfide using glutathione reductase and 2-vinylpyridine. *Anal. Biochem.* **1980**, *106*, 207–212.
(58) Griffith, O. W.; Meister, A. Potent and specific inhibition of glutathione synthesis by buthionine sulfoximine (*S*-*n*-butyl homocysteine sulfoximine). *J. Biol. Chem.* **1979**, *254*, 7558–7560.